Approximating Radiative Corrections for Analytical Applications in the Data Analysis

George Smirnov

Approximating Radiative Corrections for Analytical Applications in the Data Analysis

G.I. Smirnov

Laboratoire de Physique Corpusculaire de Clermont-Ferrand IN2P3/CNRS and
Univesité Blaise Pascal Clermont II, France

and

Laboratory of Particle Physics, JINR, Dubna, Russia.

Abstract

Exact calculations of the radiative corrections to the single spin asymmetry in the exclusive pion electroproduction below $\Delta(1232)$ resonance are performed by employing the EXCLURAD code. The analysis of the dependence of the obtained results on W, $\theta_{\rm cm}$ and ϕ shows that absolute values of radiative corrections do not exceed 1.5 %. The procedure of sampling the radiative corrections with analytical functions has been developed allowing for flexible and rapid applications of the corrections in the data analysis.

1 Introduction

Evaluation of radiative corrections (RC) to the observables of the exclusive pion electroproduction

$$e^- + p \to e^- + p + \pi^\circ \tag{1}$$

is, as a rule, performed in the framework of the approach developed in Ref. [1]. Practical calculations, which involve application of the code EXCLURAD [2], take a noticeable amount of time even in the simple case of several kinematic points. As a result, the analysis of the data registered in a wide range of kinematic variables may be hindered considerably. Approximations of the results obtained from EXCLURAD with analytical functions can substantially decrease time of the data analysis and maintain a high level of accuracy in the applied corrections. An input for the approximations is obtained by sampling of the energy and angular dependence of RC and the single spin asymmetries A and $A_{\rm RC}$ evaluated in the Born approximation and by including all relevant radiative processes, respectively.

2 Kinematics

The data on single spin asymmetry, which is observed in the reaction (1) in polarized electron beam has been collected at MAMI microtron of Mainz [3]. The relevant kinematic region is shown in Fig. 1 as a scatter plot with ten points on the $W - Q^2$ plane. Position

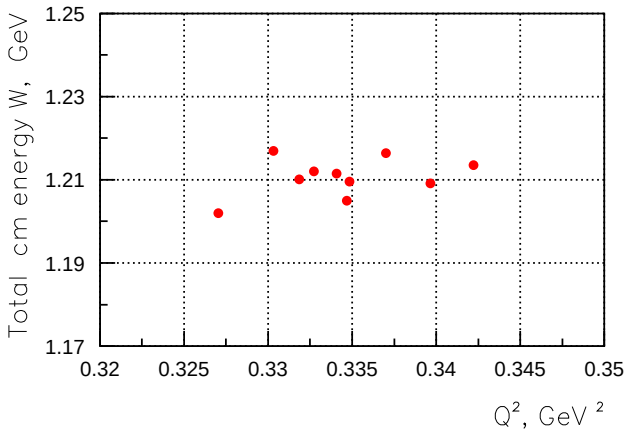

Figure 1: Location of the mean values of W and Q^2 corresponding to different experimental settings in the measurements of the single spin asymmetry at MAMI.

of the points is determined by the incident beam energy $E = 883$ MeV, and true average of each experimental bin has been found in the analysis of Ref. [4].

The code EXCLURAD computes RC to the fourfold cross section $d^4/dWdQ^2d\cos\theta_h d\phi_h$ and to polarization beam asymmetry for the reaction (1). The cm system angles θ_h and ϕ_h are between the direction of the virtual photon momentum ($\vec{q} = \vec{k}_1 - \vec{k}_2$) and momentum of the final pion. As long as a pion in reaction (1) is the undetected hadron, the angles θ_h and ϕ_h are defined with respect to the direction of $-\vec{p}\,'$, i.e. *opposite* to the recoil proton momentum [1]. In what follows these angles are denoted as $\theta_{\rm cm}$ and ϕ.

Calculations of RC, A and $A_{\rm RC}$ have been performed at the fixed value of the virtual photon transfered momentum — $Q^2 = 0.335$ GeV^2, which corresponded to the central value of the Q^2 region represented by the scatter plot in Fig. 1. With the adopted definition of ϕ, both $A(\phi)$ and $A_{\rm RC}(\phi)$ are symmetric with respect to the angle $\phi = 180^\circ$. In the experiment, $\theta_{\rm cm}$ covered the range $2.5^\circ \leq \theta_{\rm cm} \leq 37.5^\circ$, and the asymmetries were sampled in 10 points inside this interval. The sampling of the ϕ dependence has been done in 11 points inside in the interval from 0 to 180°.

As has been demonstrated in Ref. [1], the inclusive asymmetry for the reaction (1) has a nontrivial dependence on the center of mass energy W around $W \approx 1.3$ GeV where it changes sign. Therefore, for reliable evaluation of RC one has to sample a much wider range of W than that covered by average values in Fig. 1. The relevant values corresponded to $W = 1.10$, 1.15, 1.21, 1.25 and 1.30 GeV.

3 Analytical expressions approximating evaluated RC

3.1 W dependence

The Bezier curves are used as the basis for approximations of both Born asymmetry $A_0(\phi, \theta, W)$ and the asymmetry modified by the radiative effects — $A_{\rm RC}(\phi, \theta, W)$. They proved to yield a simple approximating tool in the entire range of the kinematics under consideration. In this approach the asymmetry evaluated by the EXCLURAD code in a number of fixed kinematic points is approximated as

$$A = \sum_{l=0}^{3} P_l B_l(u) \ , \tag{2}$$

where P_l are parameters of the fit and $B_l(u)$ are functions defined on the interval $\{0, 1\}$:

$$\begin{aligned} B_0 &= (1-u)^3, \\ B_1 &= 3u(1-u)^2, \\ B_2 &= 3u^2(1-u), \\ B_3 &= u^3. \end{aligned} \tag{3}$$

Due to this particular choice of functions B_l, P_0 and P_3 coincide with the values of A on the left and right boundary of the interval, respectively. Thus, it is only P_1 and P_2, which are to be determined from the fit.

When fitting W dependence of the asymmetry evaluated on the interval $\{W_{\rm min}, W_{\rm max}\}$, the following change was done:

$$u = \frac{W - W_{\rm min}}{W_{\rm max} - W_{\rm min}} \ .$$

For the applications in the Mainz experiment, u has been calculated by taking $W_{\rm min} = 1.10$ GeV and $W_{\rm max} = 1.30$ GeV.

3.2 Dependence on the azimuthal angle ϕ

Similarly to the case of W dependence, one has to change $u = \phi/180^\circ$ in Eq. (2) in the fitting of $A(\phi)$. On the other hand, one can suggest some simplifications to Eq. (2), which would better suit conditions of the Mainz experiment, in which the difference between Born and RC asymmetries is very small everywhere except of $W \sim 1.3$ GeV. This is done by noticing that $A(\phi)$ is close to a sine function and by replacing 1st and 4th terms (which have to disappear in the case of purely sine function) with a sine term:

$$A(\phi) = P_0 \sin(\phi) + P_1 B_1(u) + P_2 B_2(u), \tag{4}$$

where $u = \phi/180^\circ$. The dependence of parameters P_l on W is obtained by fitting the results with Eq. (2). The resulting 2D asymmetry is given by

$$A(\phi, W) = \sum_{l=0}^{2} B_l^\phi \sum_{m=0}^{3} P_{lm} B_m^W \ , \tag{5}$$

where $B_0^\phi = \sin(\phi)$, and $B_{1,2}^\phi$ are usual functions defined in Eq. (3).

3.3 Dependence on the angle $\theta_{\rm cm}$

As it is obtained from calculations of the $A(\theta_{\rm cm})$ by the EXCLURAD, both $A(\theta_{\rm cm})$ and $A_{\rm RC}(\theta_{\rm cm})$ are small and slowly varying functions in the kinematics covered by the experiment ($2.5^\circ \leq \theta_{\rm cm} \leq 37.5^\circ$). Therefore, the most economical way of approximating the asymmetry is the choice of the two-terms functions as follows:

$$A(\theta) = a\sin(\theta_{\rm cm}) + b\sin^2(\theta_{\rm cm}) \ . \tag{6}$$

Correspondingly, approximation of the $A(\phi, \theta_{\rm cm})$ has been performed for a given value of W in the following form:

$$A(\phi, \theta_{\rm cm}) = \sum_{l=0}^{1} (\sin(\theta_{\rm cm}))^{l+1} \sum_{m=0}^{3} P_{lm} B_m^{\phi} \ , \tag{7}$$

where functions B_m^{ϕ} are defined in Eq. (3). Parameters P_{lm} of the fit performed for the case with radiative processes are shown in Table 1.

	m = 0	m = 1	m = 2	m = 3
l = 0	–0.51822	8.2071	6.8661	–0.51799
l = 1	1.3751	–4.0265	–6.4145	1.3751

Table 1: Parameters P_{lm} that determine $A_{\rm RC}(\phi, \theta_{\rm cm})$

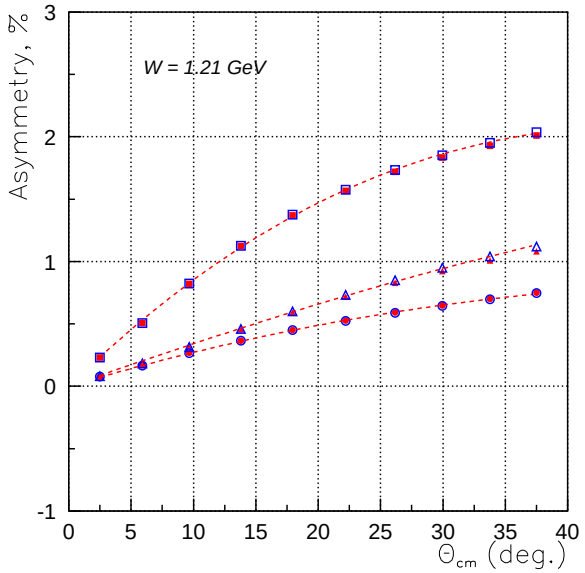

Figure 2: Asymmetry as a function of $\theta_{\rm cm}$ evaluated for three values of the azimuthal angle ϕ — 20° (triangles), 90° (squares) and 160° (circles). Asymmetries calculated in Born approximation and by accounting for radiative precesses (assuming $\Delta S = 0.02$ GeV^2) are shown with filled and open symbols, respectively.

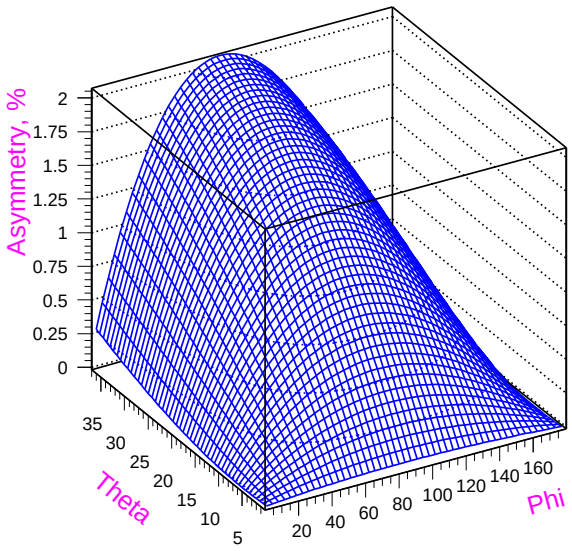

Figure 3: Asymmetry $A_{\rm RC}(\phi, \theta_{\rm cm})$ evaluated at $W = 1.21$ GeV by assuming $\Delta S = 0.02$ GeV^2.

4 Results

It was found that the modification of the asymmetry due to radiative effects in the reaction under study is the strongest at $\theta_{\rm cm} = 37.5°$. This is demonstrated by the results of calculations $A(\theta_{\rm cm})$ and $A_{\rm RC}(\theta_{\rm cm})$ shown in Fig. 2 for three values of the azimuthal angle ϕ.

Radiative corrections depend on the mass window ΔS around the missing mass peak used in the event selection procedure if $\Delta S < \nu_{\rm max}$, where $\nu_{\rm max}$ is introduced in EXCLURAD as the upper limit of integration in calculating the cross section of the radiative process. The parameter $\nu_{\rm max}$ describes the missing mass of the radiative origin (due to undetected γ). It is dubbed as "maximum inelasticity" and is defined in Ref. [1] as

$$\nu_{\rm max} \quad = (W - M_p)^2 - m^2_{\pi^\circ} \ . \tag{8}$$

Undetected gammas additionally distort the missing mass spectrum, which is of the hadronic origin (undetected π^0 in the considered case). The selection cuts, which are usually applied to the distribution of the events versus missing mass squared M_x^2, are generally more tight than $\Delta S = \nu_{\rm max}$, which is modeled in EXCLURAD by replacing the upper limit of integration with $\nu_{\rm cut}$. Accordingly, the mass window ΔS is related to $\nu_{\rm cut}$ as

$$\Delta S \quad = \nu_{\rm max} - \nu_{\rm cut} \ . \tag{9}$$

The corrections naturally increase as the cuts tighten, corresponding to narrowing of the mass window ΔS.

	m = 0	m = 1	m = 2	m = 3
l = 0	–1.4506	–4.6186	–1.9493	0.17369
l = 1	5.7645	12.049	7.0872	–2.7053
l = 2	2.4684	6.8852	8.1888	–2.6894

Table 2: Parameters P_{lm} that determine $A(\phi, W)$

The two-dimensional plot for $A_{\rm RC}(\theta_{\rm cm})$ corresponding to the case of $\Delta S = 0.02$ GeV^2 is obtained analytically by employing Eq. (7). It is displayed in Fig. 3. The difference between $A_{\rm RC}(\theta_{\rm cm})$ and $A(\theta_{\rm cm})$ is better seen from Fig. 4, which shows radiative corrections δ_A defined in Ref. [1] as

$$\delta_A = \frac{A_{\rm RC} - A}{A} \cdot 100\% \ . \tag{10}$$

The set of ten curves in Fig. 4 shows the dependence of δ_A for ten values of $\theta_{\rm cm}$ on the size of the ΔS window used in the event selection procedure. The results have been produced for the azimuthal angle $\phi = 90°$, where corrections are found to be largest.

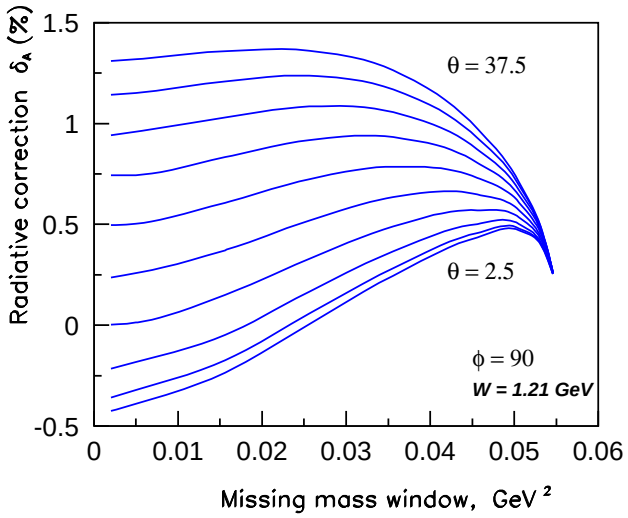

Figure 4: Radiative corrections as a function of the ΔS window evaluated in 10 points of the phase space corresponding to the angle $\theta_{\rm cm}$ in the range 2.5° – 37.5° and at the azimuthal angle $\phi = 90°$.

In this study, a larger number of results have been produced for the kinematics corresponding to $\theta_{\rm cm} = 37.5°$.

The curves in Fig. 5 represent results of the fits, in which Eq. (5) was employed. The fitting procedure started from Eq. (4) and three parameters P_l have been obtained in five points of W, which allowed to conduct a fit of the W dependence for each of them. It is realized by using Eq. (2), and Fig. 6 shows obtained parameters.

The parameters thus obtained are presented in Tables 2 and 3. They are used in Eq. (5) for rapid evaluation of $A(\phi, W)$ and $A_{\rm RC}(\phi, W)$ at the angle $\theta_{\rm cm} = 37.5°$ and the ΔS window of 0.020 GeV^2. The result is displayed in Fig. 7.

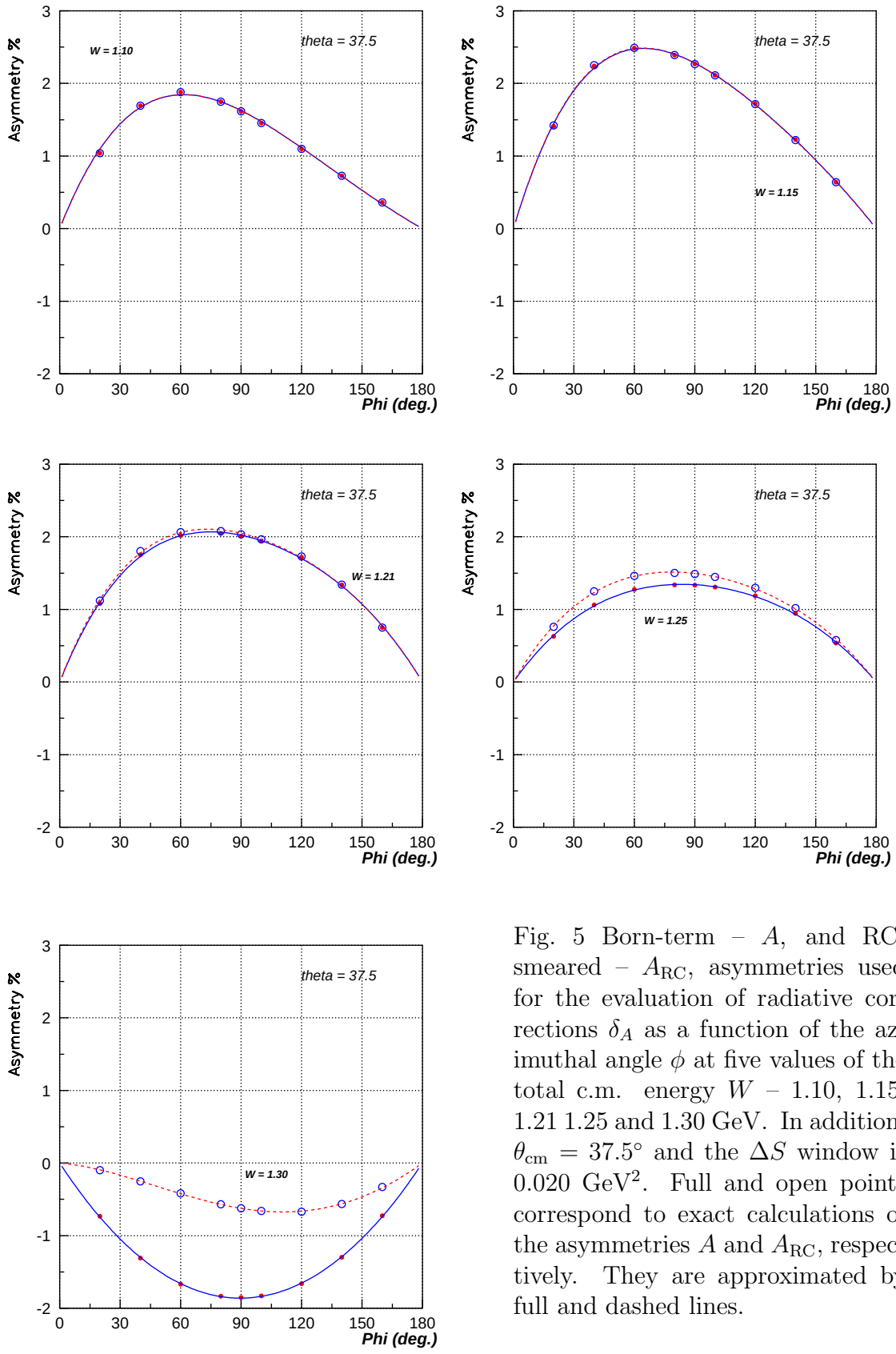

Fig. 5 Born-term – A, and RC-smeared – $A_{\rm RC}$, asymmetries used for the evaluation of radiative corrections δ_A as a function of the azimuthal angle ϕ at five values of the total c.m. energy W – 1.10, 1.15, 1.21 1.25 and 1.30 GeV. In addition, $\theta_{\rm cm} = 37.5°$ and the ΔS window is 0.020 GeV^2. Full and open points correspond to exact calculations of the asymmetries A and $A_{\rm RC}$, respectively. They are approximated by full and dashed lines.

	m = 0	m = 1	m = 2	m = 3
l = 0	–1.4544	–4.6810	–2.2870	–0.54204
l = 1	5.7668	12.365	6.2068	0.45351
l = 2	2.4694	7.1451	7.6380	–0.64024

Table 3: Parameters P_{lm} that determine $A_{\rm RC}(\phi, W)$

	m = 0	m = 1	m = 2	m = 3
l = 0	–1.4544	–4.6810	–2.2870	–0.54204
l = 1	5.7668	12.365	6.2068	0.45351
l = 2	2.4694	7.1451	7.6380	–0.64024

Table 4: Parameters P_{lm} that determine $A_{\rm RC}(\phi, W)$

Dependence of the additive correction defined as $A - A_{\rm RC}$ on ϕ and W is shown in Fig. 8 for the same conditions as in Fig. 7. As it is demonstrated by Fig. 2, the asymmetries

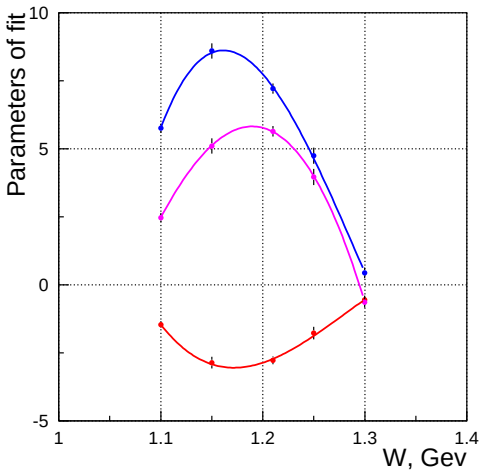

Figure 6: W dependence of parameters P_l of Eq. (3) evaluated for Born asymmetry at $\theta_{\rm cm} = 37.5°$. Three curves (from top to bottom) correspond to P_1, P_2 and P_0.

$A(\phi, \theta_{\rm cm})$ and $A_{\rm RC}(\phi, \theta_{\rm cm})$ are slow varying functions of $\theta_{\rm cm}$, which reach maximum at the end of the considered kinematic interval – $\theta_{\rm cm} = 37.5°$. This feature justifies an approximate sampling of asymmetries for any given value of $\theta_{\rm cm}$ by scaling down the asymmetry found for $\theta_{\rm cm} = 37.5°$. To this end, one can construct a normalizing function $f_N(\phi, \theta_{cm})$

$$f_N(\phi, \theta_{\rm cm}) = \frac{A(\phi, \theta_{\rm cm})}{A(\phi, \theta_{\rm cm}^{\rm max})} \ , \tag{11}$$

where $A(\phi, \theta_{\rm cm})$ is defined by Eq. (7), and $A(\phi, \theta_{\rm cm}^{\rm max})$ corresponds to the results of the fit at $\theta_{\rm cm} = 37.5°$. The combination of $f_N(\phi, \theta_{\rm cm})$ with the results given by Eq. (5) provides a simple and precise tool for evaluating $A(\phi, W, \theta_{\rm cm})$ in the region around $W = 1.2$ GeV:

$$A(\phi, W, \theta_{\rm cm}) = A(\phi, W) f_N(\phi, \theta_{\rm cm}). \tag{12}$$

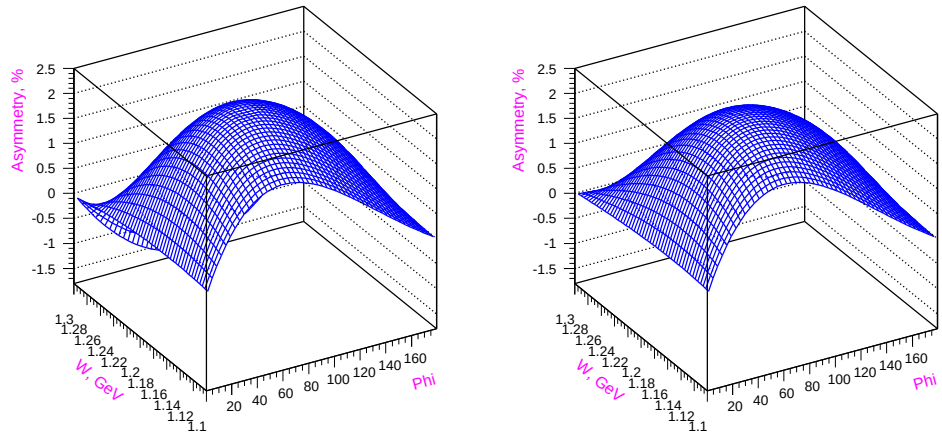

Figure 7: Single spin Born asymmetry $A(\phi, W)$ (left panel) and the asymmetry $A_{\rm RC}(\phi, W)$ modified by radiative effects (right panel), both evaluated for $\theta_{\rm cm} = 37.5^\circ$.

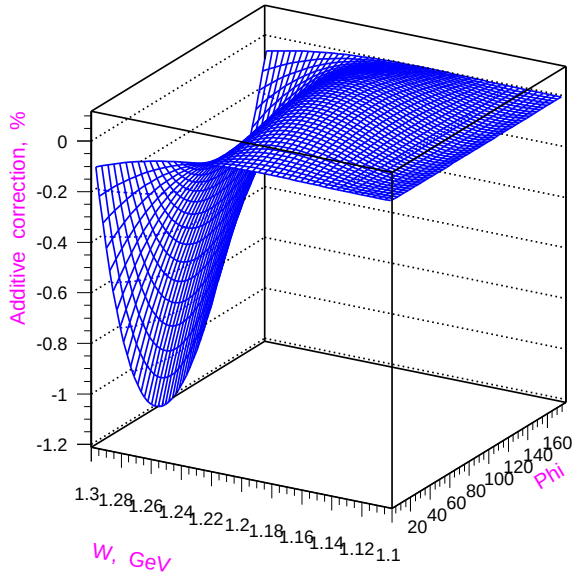

Figure 8: Additive correction obtained as $A - A_{\rm RC}$, which corresponds to the difference between the plots in the left and right panels of Fig. 7.

Two dimensional plots for $A_{\rm RC}(\phi, W)$ evaluated by employing this approximation are displayed in Fig. 9.

For practical applications the window size ΔS was varied in RC calculations between 0.005 and 0.020 GeV^2. In some plots (e.g. in Fig. 10), for illustration purposes, the window size has been increased up to 0.078 GeV^2. In the kinematics under study (this time calculations were done at $W = 1.25$ GeV), the use of such wide window in the event selection serves an educative purpose: it allows to keep virtually all events and obtain the asymmetry, which coincides with the Born one. The considered in Fig. 10 case corresponds to rather large phase space of emission of a bremsstrahlung photon. The phase space rapidly contracts when W approaches the lower boundary of the kinematic region. Therefore, at $W = 1.1$ GeV all radiatively distorted events can be found inside rather small window of 0.005 GeV^2. On the contrary, as W approaches 1.3 GeV, application of the event selection procedure within windows from 0.005 to 0.024 GeV^2, which is a typical size in the data analysis, results in a selection of certain parts of the event samples, which have the following properties that can be traced in Fig. 4:

(1)	Large $\theta_{\rm cm}$	$\rightarrow$	Large RC	$\rightarrow$	No dependence on window size
(2)	Small $\theta_{\rm cm}$	$\rightarrow$	Small RC	$\rightarrow$	Certain dependence on window size

Accordingly, when $(\Delta W)^2$ approaches its maximum value, the corrections vanish, which is seen from converging of curves in Fig. 4 to a single point $\delta_A = 0$, and also from convergence of measured and Born asymmetries displayed in Fig. 10.

5 Summary

In the kinematics of the considered experiment, the radiative effects that manifest themselves in the observed single spin asymmetry are largest at $W = 1.3$ GeV and at the $\theta_{\rm cm} = 37.5^\circ$. But even there they do not change the Born asymmetry by more than 1.0 – 1.5 % (in absolute value). A monotonous rise of $A(\theta_{\rm cm})$ and $A_{\rm RC}(\theta_{\rm cm})$ in the angular interval (0, 37.5°) allows to employ simple analytical approximation of the asymmetries and radiative corrections by evaluating them in the maximum ($\theta_{\rm cm}^{\rm max} = 37.5^\circ$) and scaling down to any value of $\theta_{\rm cm}$ inside the considered interval. A number of analytical functions, which approximate numerical results from EXCLURAD, offer flexible tools for fast applications of radiative corrections as a function of W, $\theta_{\rm cm}$ and ϕ.

The dependence of radiative corrections on the ΔS window, if it is chosen as $0.005 < \Delta S < 0.024$ GeV^2, can be neglected in the whole range of W but from the very different grounds: (1) at $W = 1.1$ GeV any ΔS window completely covers the phase space of radiative events, (2) at $W = 1.3$ GeV any ΔS window is small compared to the phase space of radiative events, but falls onto the plateau of the dependence of the radiative corrections on the ΔS window size.

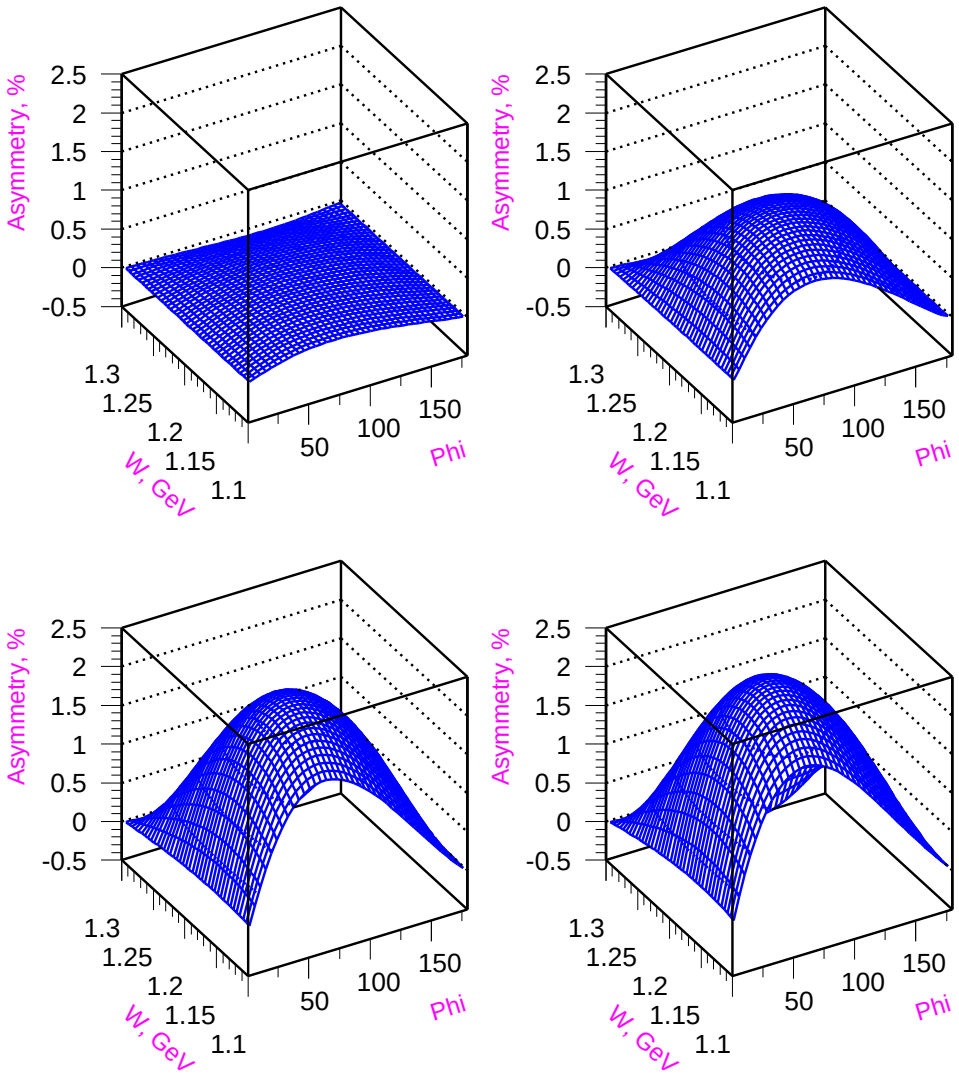

Figure 9: Single spin asymmetry $A_{\rm RC}(\phi, W)$, which includes radiative effects evaluated for the values of the polar angle $\theta_{\rm cm} = 2.5^\circ$ (upper left), 13.8° (upper right), 30° (lower left) and 37.5° (lower right).

6 Acknowledgments

I have benefited from fruitful discussions with H. Fonvieille and A. Afanasev. I am grateful to University of Blaise Pascal Clermont-Ferrand II for kind hospitality during my work on this project.

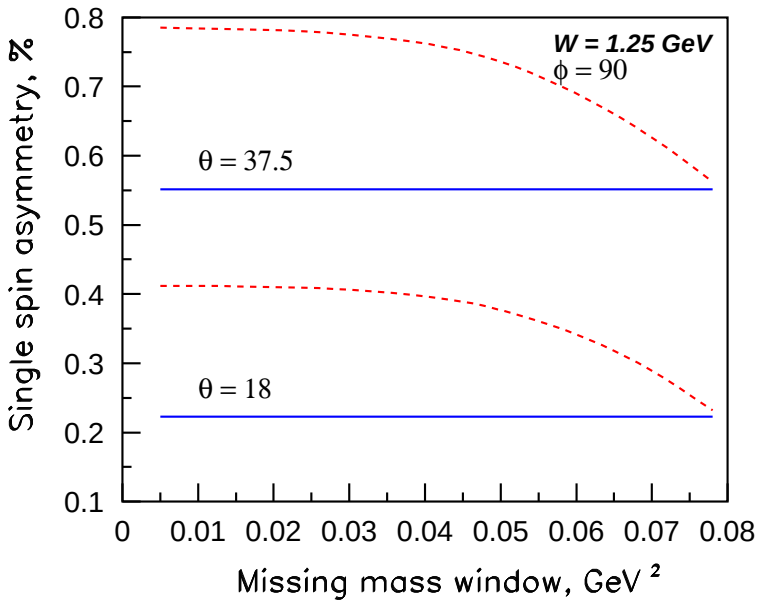

Figure 10: Single spin asymmetry as a function of the ΔS window evaluated at two data points corresponding to the angles $\theta_{\rm cm} = 18°$ and 37.5°. Full and dashed lines show A and $A_{\rm RC}$, which are the Born term and smeared by radiative effects asymmetries, respectively.

7 Appendix

This section explains how the Fortran functions written for the approximation of the single spin asymmetries and radiative corrections can be used in practical work.

All asymmetries approximated by the functions correspond to the MAID-2000 parameters used as the input for EXCLURAD.

The arguments of the functions are in units of "GeV" (for the total c.m. energy W) and "degree" (for angles $\theta_{\rm cm}$ and ϕ).

1. FBORNA(PHI,W)
   Returns asymmetry $A(\phi, W)$ (%) in Born approximation at fixed $\theta_{\rm cm} = 37.5°$.
   It has been used in producing left-panel plot of Fig. 7.

2. FRC020(PHI,W)
   Returns asymmetry $A_{\rm RC}(\phi, W)$ (%), which includes radiative effects, at fixed $\theta_{\rm cm}$ = 37.5° and corresponds to the event selection in the missing mass window of 0.02 GeV^2.
   It has been used in producing right-panel plot of Fig. 7 as well as lower-right plot in Fig. 9.

3. VRADCOR(PHI,W)
   Returns correction obtained by subtracting asymmetry $A_{\rm RC}(\phi, W)$ from Born asymmetry $A(\phi, W)$. Uses functions FBORNA(PHI,W) and FRC020(PHI,W).
   It has been used in producing the plot in Fig. 8.

4. FASYMT(PHI,TH)
   Returns $A_{\rm RC}(\phi, \theta)$ (%) at fixed $W = 1.21$ GeV and corresponds to the event selection in the missing mass window of 0.02 GeV^2.
   It has been used in producing the plot in Fig. 3.

5. FNORM(PHI,TH)
   Returns the ratio of $A_{\rm RC}(\phi, \theta_{\rm cm})$ and $A_{\rm RC}(\phi, \theta_{\rm cm}^{\rm max})$ for any given $\theta_{\rm cm}$ in the W region around the mean value of the considered experiment – $W \approx 1.2$ GeV. It has the same structure and uses the same set of fit parameters as the function FASYMT(PHI,TH).
   It has been used in producing the plots in Fig. 9.

References

[1] A. Afanasev, I. Akushevich, V. Burkert and K. Joo, Phys. Rev. D **66**, 074004 (2002).

[2] A. Afanasev, I. Akushevich, V. Burkert and K. Joo, EXCLURAD code, http://www.jlab.org/RC/.

[3] H. Merkel and N. D'Hose — spokespersons, MAMI Proposal, Mainz, 2000.

[4] H. Fonvieille and I. Bensafa, Private communication, Clermont-Ferrand.

[5] D. Drechsel, O. Hanstein, S. Kamalov and L. Tiator, Nucl. Phys. A**645** (1999) 145.